

1 Genomic Analysis of Hypoxia Inducible Factor Alpha Evolution in Ray-finned Fishes

2 (Actinopterygii)

3

4 Ian K. Townley¹ and Bernard B. Rees²

5

6 ¹Department of Cell and Molecular Biology

7 Tulane University

8 New Orleans, LA 70118

9

10 ²Department of Biological Sciences

11 University of New Orleans

12 New Orleans, LA 70148

13

14 Corresponding author: Bernard B. Rees, brees@uno.edu

15

16

17 Significance statement: Vertebrate animals have multiple copies of the hypoxia inducible

18 transcription factor, a critical regulator of oxygen-dependent gene expression, but the number of

19 copies in fishes and their relationships are incompletely understood. This study mines the

20 genomes of ray-finned fishes, finds evidence of gene duplicates not previously appreciated, and

21 clarifies the relationships among duplicates that arose early in vertebrate evolution and those

22 arising from later rounds of genome duplication in fishes.

23 Abstract: Two rounds of genome duplication (GD) in the ancestor of vertebrates, followed by
24 additional GD during the evolution of ray-finned fishes (Actinopterygii), expanded certain gene
25 families, including those encoding the hypoxia inducible transcription factor (HIF). The present
26 study analyzed Actinopterygian genomes for duplicates of HIF α , the subunit that confers
27 oxygen-dependent gene regulation. In contrast to tetrapod vertebrates that retain three HIF α
28 genes from the ancestral vertebrate GD, four HIF α forms were found in the genomes of primitive
29 Actinopterygians (spotted gar and Asian arowana). All four forms have been retained in
30 zebrafish and related species (Otocephala) and salmonids and their sister taxa (northern pike) but
31 one of them (HIF4 α) was lost during the evolution of more derived fishes (Neoteleostei). In
32 addition, the current analyses confirm that Otocephala retain duplicates of HIF1 α and HIF2 α
33 from the teleost-specific GD, provide new evidence of salmonid-specific duplicates of HIF1 α ,
34 HIF2 α , and HIF3 α , and reveal a broad distribution of a truncated form of HIF2 α in salmonids
35 and Neoteleostei. This study delivers a comprehensive view of HIF α evolution in the ray-finned
36 fishes, highlights the need for a consistent nomenclature, and suggests avenues for future
37 research on this critical transcription factor.

38

39

40

41

42

43 Keywords: genome duplication, ohnolog, phylogenetic analysis, shared synteny, teleost

44 evolution, transcription factor

45 Introduction

46 Species richness and ecological diversity of the teleost fishes have been attributed, in part, to the
47 evolutionary potential that ensued from multiple genome duplication (GD) events that occurred
48 during the evolution of this group (Volff 2005; Glasauer and Neuhauss 2014; Guo 2017; Ravi
49 and Venkatesh 2018). Two GD occurred at the base of vertebrate evolution (Ohno 1970; Dehal
50 and Boore 2005; Sacerdot et al. 2018), and the evolution of ray-finned fishes (Actinopterygii),
51 which comprise about half of the extant species of vertebrate animals, has been characterized by
52 additional GD: the teleost-specific genome duplication (TGD) occurred early in the evolution of
53 teleost fishes (Postlethwait et al. 2000; Volff 2005; Pasquier et al. 2016; Ravi and Venkatesh
54 2018) and a more recent GD occurred during the evolution of salmonids (SGD) (Berthelot et al.
55 2014; Macqueen and Johnston 2014). Although the most common fate of gene duplication is
56 silencing of one copy (nonfunctionalization) (Lynch and Conery 2000; Inoue et al. 2015), a
57 considerable number of duplicates can be maintained by acquiring a new function
58 (neofunctionalization) or by sharing the roles, developmental timing, or tissue specificity of the
59 ancestral gene (subfunctionalization) (Force et al. 1999). Indeed, genomic analyses of teleost
60 fishes shows a high proportion of gene duplicates have been maintained in certain species (e.g.,
61 up to 48% in rainbow trout; Berthelot et al. 2014).

62 The hypoxia-inducible factor (HIF) orchestrates cellular responses to low oxygen in
63 animals (Kaelin and Ratcliffe 2008; Semenza 2011). The active transcription factor is composed
64 of an oxygen-dependent alpha subunit (HIF α) and a constitutively expressed beta subunit (HIF β),
65 also known as the aryl hydrocarbon receptor nuclear translocator (ARNT), both of which belong
66 to the large family of PAS-domain proteins, so named for conserved domains present in the
67 transcription factors Period, ARNT, and Single-minded (Gu et al. 2000; McIntosh et al. 2010).

68 Tetrapod vertebrates, including humans, have three forms of HIF α encoded by the *HIF1A*,
69 *HIF2A*, and *HIF3A* loci (see Box 1, Supplementary Material online)(Kaelin and Ratcliffe 2008;
70 Semenza 2011; Duan 2016). Previous analyses of HIF α evolution among fishes suggested that
71 most teleost fishes have three forms, which appear to be orthologs of the forms found in
72 tetrapods (Nikinmaa and Rees 2005; Rytönen et al. 2011; Rytönen et al. 2013; Townley et al.
73 2017). However, zebrafish and relatives (*Cyprinidae*) possess six forms and some non-cyprinid
74 species retain a truncated form of HIF2 α (Rytönen et al. 2013; Graham and Presnell 2017;
75 Townley et al. 2017). Rytönen et al. (2013, 2014) provided evidence that the six forms in
76 *Cyprinidae* arose from the TGD and were maintained in this lineage by subfunctionalization,
77 whereas they were lost, or dramatically truncated, in other lineages.

78 Here, we reexamined the evolution of HIF α in ray-finned fishes using recently sequenced
79 genomes, including that of spotted gar (*Lepiosteus oculatus*) to represent a lineage that diverged
80 prior to the TGD (Braasch et al. 2016). Specifically, we sought to determine (1) whether any ray-
81 finned fishes retained the four HIF α genes that arose during the two rounds of GD at the base of
82 vertebrate evolution, (2) whether gene duplicates arising from the TGD are seen in fishes other
83 than the *Cyprinidae*, (3) whether HIF α duplicates from the SGD are present in salmonid
84 genomes, and (4) the phylogenetic relationship and distribution of shortened forms of HIF2 α .

85

86 Methods

87 Actinopterygian genomes at NCBI (<https://www.ncbi.nlm.nih.gov>) or Ensemble
88 (<http://www.ensembl.org/>) were searched for HIF α genes through June 2020. The corresponding
89 coding sequences (CDS) were checked to ensure each was complete and, when multiple CDSs
90 were available for a single locus, the longest sequence was retained. The final sequence list was

91 curated to avoid overrepresentation of Neoteleostei and to remove sequences with poor
92 chromosomal or linkage group assignment (supplementary table S1, Supplementary Material
93 online).

94 Multiple sequence alignments (MSA) were made using MAFFT version 7.123b (Katoh
95 and Standley 2013; Katoh and Standley 2016) implemented through the GUIDENCE2 server
96 with Max-iterate of 20 (<http://guidance.tau.ac.il/ver2/>). For phylogenetic analysis, we used the
97 MSA with the default column cutoff of below 0.93 (Penn et al. 2010; Sela et al. 2015). Bayesian
98 analyses were performed in BEAST 2 v2.6.1 (<https://www.beast2.org/>) applying an uncorrelated
99 log normal relaxed molecular clock model (Drummond et al. 2006), a Yule model prior, with
100 10,000,000 chain-length and 100,000 burn-in (Drummond et al. 2012; Bouckaert et al. 2014).
101 Nucleotide analysis employed a general time reversible codon substitution model allowing for
102 invariants and six gamma categories (GTR+I+G). Amino acid analysis employed a JTT matrix-
103 based model (Jones et al. 1992) allowing for invariants and six gamma categories. The maximum
104 clade credibility tree was selected using TreeAnnotator v2.6.0. Maximum likelihood analyses
105 were performed using MEGAX v10.1.8 (Kumar et al. 2018) with 100 bootstrap replicates
106 (Felsenstein 1985) under the same conditions used in Bayesian analyses. The trees with the
107 highest log likelihood were visualized and edited in FigTree v1.4.4
108 (<http://tree.bio.ed.ac.uk/software/figtree/>).

109 Shared synteny among representative species was assessed by determining the flanking
110 deduced open reading frames (ORF) using the NCBI Graphical Sequence Viewer (v3.38.0). If a
111 putative ORF lacked a clear identification, BLASTP was used to compare the deduced protein
112 sequence against Actinopterygii. A small number of putative ORFs could not be identified and
113 were kept in the analysis as “unknowns”. For genes lacking an abbreviation at NCBI, the gene

114 name was used in a search of UniprotKB (<https://www.uniprot.org>), and the corresponding
115 abbreviation was used.

116 The N-and C- terminal oxygen-dependent degradation domains (NODD and CODD) and
117 the C-terminal asparaginyl hydroxylation motif (CEVN) were identified from multiple sequence
118 alignments in Jalview v2.10.5 (Waterhouse et al. 2009). The NODD and CODD included the
119 canonical LxxLAP sequence targeted by prolyl hydroxylases and adjacent residues known to
120 play a role in oxygen-dependent regulation of HIF α (Tarade et al. 2019). Consensus sequences
121 were made using the Skylign server (<http://skylign.org/>) (Wheeler et al. 2014).

122

123 Results and Discussion

124 Phylogenetic analyses of 114 putative HIF α homologs from 22 species in 14 orders of
125 Actinopterygii (supplementary table S1, Supplementary Material online) resolved four distinct
126 homology groups (fig. 1). This pattern was strongly supported by Bayesian analyses of
127 nucleotide and deduced amino acid sequences (posterior probabilities ≥ 0.89 ; supplementary
128 figs. S1, S3, Supplementary Material online), as well as by maximum likelihood (bootstrap
129 values ≥ 0.71 for nucleotide analyses and ≥ 0.79 for amino acid analyses; supplementary figs.
130 S2, S4, Supplementary Material online). The branching patterns of species within each
131 homology group generally reflected the known phylogeny of fishes (Hughes et al. 2018),
132 although the relationship of paralogs varied among analyses (see below).

133 The spotted gar (*Lepiosteus oculatus*), a basal Actinopterygian that diverged prior to the
134 TGD, has one homolog in each group. Thus, we infer that the four groups represent products of
135 the two rounds of GD in the ancestor of vertebrates (i.e., ohnologs, Ohno 1970; Wolfe 2000) and
136 hereafter refer to these as HIF1 α , HIF2 α , HIF3 α , and HIF4 α . The current results support

137 previous observations (Graham and Presnell 2017) and suggest that several sequences described
138 as “HIF α -like” are HIF3 α or HIF4 α (fig. 1, supplementary table S1, Supplementary Material
139 online). Like the spotted gar, the Asian arowana (*Scleropages formosus*) has four HIF α genes,
140 one in each of the major groups. The arowana is in the Osteoglossiformes (bonytongues), an
141 ancient order that diverged early from the main branch of teleost evolution (Hughes et al. 2018),
142 but after the TGD (Bian et al. 2016). In this lineage, therefore, one of each pair of HIF α paralogs
143 resulting from the TGD appears to have been lost due to nonfunctionalization, as predicted for
144 other TGD paralogs (Bian et al. 2016).

145 Our analysis confirms that Cypriniformes (e.g., zebrafish and common carp) have
146 duplicated forms of HIF1 α (HIF1 α a and HIF1 α b) and HIF2 α (HIF2 α a and HIF2 α b), which likely
147 arose during the TGD (Rytkönen et al. 2013). These duplicates are more broadly distributed than
148 previously appreciated, being present in all the species in Otocephala that were examined,
149 including Atlantic herring, Mexican tetra, and channel catfish. More derived fishes appear to lack
150 HIF1 α b, although a truncated version of HIF2 α has been retained (see below; Rytkönen et al.
151 2013). Otocephala has two other HIF α forms that group with HIF3 α and HIF4 α from spotted gar.
152 This placement strongly suggests that these forms represent ohnologs arising from the GD in
153 ancestral vertebrates, rather than HIF3 α duplicates arising from the TGD, as previously proposed
154 (Rytkönen et al. 2013).

155 The current analysis revealed that Salmoniformes have two forms of HIF1 α , HIF2 α , and
156 HIF3 α (fig. 1). These duplicates are not observed in the sister group Esociformes (pike) and the
157 branch lengths joining them are very short, consistent with an origin during the SGD. Berthelot
158 et al. (2014) noted that rainbow trout retained as many as 48% of the gene duplicates, including
159 an over-representation of transcription factors. Because salmonids generally occur in well-

160 oxygenated habitats and have poor hypoxia tolerance, there is no apparent link between HIF α
161 duplication and hypoxia tolerance in this group. Rather, these duplicates may play other roles in
162 salmonid physiology or life-history. Alternatively, duplicates may be destined for
163 nonfunctionalization, a process that is likely still underway in this lineage (Berthelot et al. 2014).
164 Only one salmonid-specific duplicate of HIF4 α was recovered in the current analysis, suggesting
165 one duplicate has already been nonfunctionalized. In addition, HIF4 α appears to be completely
166 absent in more derived fishes (Neoteleostei).

167 Genomic analysis also supports the broad distribution of a truncated form of HIF2 α ,
168 occurring in Salmoniformes and all Neoteleostei examined. The deduced protein sequence
169 corresponds to the N-terminal half of HIF2 α , containing the basic helix-loop-helix and PAS
170 domains, which are important for DNA-binding and protein dimerization, but lacking sites for
171 oxygen-dependent regulation of protein stability and gene activation (Rytkönen et al. 2013;
172 Townley et al. 2017). Although speculative, this truncated form of HIF2 α might act as a negative
173 regulator by dimerizing with other HIF α subunits and preventing their transcriptional activity, as
174 demonstrated for similarly truncated forms of HIF3 α that arise from alternative splicing in
175 mammals (Makino et al. 2002). Alternatively, this form may be undergoing
176 nonfunctionalization, particularly in Salmoniformes in which even shorter forms are present in
177 species not included in this genomic analysis.

178 Because the relationship of paralogs arising from the TGD based upon sequence analyses
179 alone can be ambiguous (supplementary figs. S1-S4, Supplementary Material online; Parey et al.
180 2020), we used shared synteny among species representing major fish lineages to clarify the
181 relationships among HIF α paralogs (fig. 2; supplementary table S2, Supplementary Material
182 online). For HIF1 α , several flanking genes are conserved from spotted gar (*L. oculatus*) through

183 Neoteleost (represented by *X. maculata*). A subset of up to eight neighboring genes is shared
184 among HIF1 α a in Otocephala (represented by *D. rerio*) and HIF1 α in other fishes, but not found
185 for Otocephala HIF1 α b. This pattern supports the view that HIF1 α a of Otocephala is orthologous
186 with HIF1 α in other fishes, whereas HIF1 α b was lost in those lineages (Rytönen et al. 2013).

187 Although the ancestral gene order flanking HIF2 α is not as highly conserved across
188 species, up to 10 genes are shared among one of the forms found in Otocephala and the truncated
189 form found in more derived species (yellow arrows, fig. 2B). Rytönen et al. (2013) originally
190 proposed that this form be recognized as HIF2 α b, a convention we previously endorsed
191 (Townley et al. 2017) and maintain here (supplementary table S1, Supplementary Material
192 online). Thus, the other paralog, which includes the first, full-length HIF2 α described in fishes
193 (Powell and Hahn 2002; Rojas et al. 2007), corresponds to HIF2 α a. In current databases,
194 however, the names of HIF2 α paralogs are reversed: that is, the full-length and presumably
195 functional form of HIF2 α is listed as *hif2ab* or *epas1b*, whereas the other form, which is
196 truncated in most fishes, is *hif2aa* or *epas1a*. Until there is consensus, great care will be needed
197 when interpreting reports of paralog-specific differences in HIF2 α .

198 Mining of fish genomes yielded only one form of HIF3 α and HIF4 α , and the latter was
199 completely missing in more derived fishes (see above). The most parsimonious evolutionary
200 scenario is that one paralog of each gene was lost shortly after the TGD, with the remaining form
201 of HIF4 α subsequently lost in Neoteleost (fig. 2C, D). An alternative hypothesis is that different
202 teleost lineages retained different paralogs after the TGD (i.e., divergent silencing; Lynch 2002).
203 This possibility is supported by the strong conservation of gene order flanking HIF3 α within
204 Otocephala, with very little shared synteny between Otocephala and other teleost lineages (fig

205 2C; supplemental table S2, Supplementary Material online). Further analyses will be required to
206 confidently assign orthology of HIF3 α and HIF4 α in extant fishes.

207 As mentioned above, Salmoniformes have duplicates of HIF1 α , HIF2 α , and HIF3 α
208 arising from the SGD. We tentatively group these as “s1” and “s2” based upon sequence
209 similarity within Salmoniformes and the observation that one of these (s1) shows greater shared
210 synteny with the corresponding gene in Esociformes, the sister group of Salmoniformes
211 (supplementary table S2, Supplementary Material online).

212 Among all species examined, the number of exons and length of deduced proteins are
213 highly conserved within each HIF α type, with the notable exception of the truncated form,
214 HIF2 α b (fig. 3A, B; supplementary table S3 Supplementary Material online). We also analyzed
215 variation in the amino acid sequences of putative functional domains, including the N-terminal
216 and C-terminal oxygen dependent degradation domains (NODD and CODD) that are potential
217 targets of regulation by prolyl hydroxylases (Epstein et al. 2001) and the extreme C-terminal
218 CEVN motif targeted by asparaginyl hydroxylase (Lando et al. 2002) (fig. 3C). In general, the
219 CODD is more highly conserved than the NODD, which is absent in HIF4 α . These observations
220 support suggestions that the CODD is more critical in determining the oxygen-dependence of
221 HIF α subunit degradation (Epstein et al. 2001; Zhang et al. 2014). Within the CODD, however,
222 sequence variation among forms of HIF α may be a source of functional divergence among
223 ohnologs. For example, M_{n-3} is found in HIF1 α and HIF3 α and G_{n+6} is found in HIF2 α and
224 HIF4 α (where n is the P that is putatively hydroxylated), and both residues are important in
225 mediating HIF α degradation (Tarade et al. 2019). Finally, the lack of the CEVN sequence in
226 HIF3 α (Gu et al. 1998; Duan 2016) and lack of the critical asparagine in salmonid HIF4 α
227 suggests that these subunits are not subject to regulation by asparaginyl hydroxylation.

228 Conclusions

229 Here, we provide evidence that basal Actinopterygians retain four copies of HIF α that arose from
230 the two rounds of GD at the base of vertebrate evolution. We advocate that a growing number of
231 “HIF α -like” genes be recognized as HIF3 α or HIF4 α , as deduced by sequence analysis and
232 shared synteny. The TGD and SGD in more derived fishes, followed by gene truncation and
233 losses, resulted in the current diversity of HIF α among ray-finned fishes. Future research may
234 better define the phylogenetic distribution and timing of gene loss events and determine whether
235 different fish lineages retained different paralogs of HIF3 α and HIF4 α . In addition, functional
236 analyses of HIF α paralogs, including truncated forms of HIF2 α b, could illuminate the
237 contribution of these duplicates to the oxygen relations and the general biology of ray-finned
238 fishes. Hypotheses that the presence of gene duplicates confers enhanced tolerance of hypoxia,
239 for example in cyprinids, should be re-examined in light of gene duplicates in closely related
240 taxa (e.g., herring) or separate lineages (e.g., Salmoniformes) that are not particularly tolerant of
241 low oxygen. It is plausible that these transcription factor duplicates have taken on functions apart
242 from oxygen regulated gene expression (neofunctionalization) that may have contributed to the
243 evolutionary and ecological success of Actinopterygii.

244

245 Acknowledgements: We thank Jenna D. Hill and Nicholas J. Vogler for assistance in the initial
246 stages of database searching and conserved domain analysis, respectively. We thank Drs. James
247 Grady (University of New Orleans), Mark Hahn, Sibel Karchner (Woods Hole Oceanographic
248 Institution), and Li Zhao (Rockefeller University) for constructive comments on this manuscript.
249 This work was supported by the Greater New Orleans Foundation.

250

251 Data Availability Statement: The data underlying this article are available at the National Center
252 for Biotechnology Information at <https://www.ncbi.nlm.nih.gov/> or at Ensembl at [https://](https://ensembl.org/index.html)
253 ensembl.org/index.html. All gene identification, mRNA, and protein accession numbers are
254 provided in supplementary table S1, Supplementary Material online.

255 References

- 256 Berthelot C, Brunet F, Chalopin D, Juanchich A, Bernard M, Noël B, Bento P, Da Silva C,
257 Labadie K, Alberti A, et al. 2014. The rainbow trout genome provides novel insights into
258 evolution after whole-genome duplication in vertebrates. *Nat Commun.* 5:3657.
259 doi:10.1038/ncomms4657.
- 260 Bian C, Hu Y, Ravi V, Kuznetsova IS, Shen X, Mu X, Sun Y, You X, Li J, Li X, et al. 2016. The
261 Asian arowana (*Scleropages formosus*) genome provides new insights into the evolution of an
262 early lineage of teleosts. *Sci Rep.* 6:24501. doi:10.1038/srep24501.
- 263 Bouckaert R, Heled J, Kühnert D, Vaughan T, Wu C-H, Xie D, Suchard MA, Rambaut A,
264 Drummond AJ. 2014. BEAST 2: A software platform for bayesian evolutionary analysis. *PLOS*
265 *Comput Biol.* 10(4):e1003537. doi:10.1371/journal.pcbi.1003537.
- 266 Braasch I, Gehrke AR, Smith JJ, Kawasaki K, Manousaki T, Pasquier J, Amores A, Desvignes
267 T, Batzel P, Catchen J, et al. 2016. The spotted gar genome illuminates vertebrate evolution and
268 facilitates human-teleost comparisons. *Nat Genet.* 48(4):427–437. doi:10.1038/ng.3526.
- 269 Dehal P, Boore JL. 2005. Two rounds of whole genome duplication in the ancestral vertebrate.
270 *PLOS Biol.* 3(10):e314. doi:10.1371/journal.pbio.0030314.
- 271 Drummond AJ, Ho SYW, Phillips MJ, Rambaut A. 2006. Relaxed Phylogenetics and Dating
272 with Confidence. *PLOS Biol.* 4(5):e88. doi:10.1371/journal.pbio.0040088.
- 273 Drummond AJ, Suchard MA, Xie D, Rambaut A. 2012. Bayesian Phylogenetics with BEAUti
274 and the BEAST 1.7. *Mol Biol Evol.* 29(8):1969–1973. doi:10.1093/molbev/mss075.
- 275 Duan C. 2016. Hypoxia-inducible factor 3 biology: complexities and emerging themes. *Am J*
276 *Physiol Cell Physiol.* 310(4):C260-269. doi:10.1152/ajpcell.00315.2015.
- 277 Epstein AC, Gleadle JM, McNeill LA, Hewitson KS, O'Rourke J, Mole DR, Mukherji M,
278 Metzen E, Wilson MI, Dhanda A, et al. 2001. *C. elegans* EGL-9 and mammalian homologs
279 define a family of dioxygenases that regulate HIF by prolyl hydroxylation. *Cell.* 107(1):43–54.
280 doi:10.1016/s0092-8674(01)00507-4.
- 281 Felsenstein J. 1985. Confidence Limits on Phylogenies: An Approach Using the Bootstrap.
282 *Evolution.* 39(4):783–791. doi:10.1111/j.1558-5646.1985.tb00420.x.
- 283 Force A, Lynch M, Pickett FB, Amores A, Yan YL, Postlethwait J. 1999. Preservation of
284 duplicate genes by complementary, degenerative mutations. *Genetics.* 151(4):1531–1545.
- 285 Glasauer SMK, Neuhauss SCF. 2014. Whole-genome duplication in teleost fishes and its
286 evolutionary consequences. *Mol Genet Genomics MGG.* 289(6):1045–1060.
287 doi:10.1007/s00438-014-0889-2.

- 288 Graham AM, Presnell JS. 2017. Hypoxia Inducible Factor (HIF) transcription factor family
289 expansion, diversification, divergence and selection in eukaryotes. *PloS One*. 12(6):e0179545.
290 doi:10.1371/journal.pone.0179545.
- 291 Gu YZ, Hogenesch JB, Bradfield CA. 2000. The PAS superfamily: sensors of environmental and
292 developmental signals. *Annu Rev Pharmacol Toxicol*. 40:519–561.
293 doi:10.1146/annurev.pharmtox.40.1.519.
- 294 Gu Y-Z, Moran SM, Hogenesch JB, Wartman L, Bradfield CA. 1998. Molecular characterization
295 and chromosomal localization of a third α -class hypoxia inducible factor subunit, HIF3 α . *Gene*
296 *Expr*. 7(3):205–213.
- 297 Guo B. 2017. Complex genes are preferentially retained after whole-genome duplication in
298 teleost fish. *J Mol Evol*. 84(5–6):253–258. doi:10.1007/s00239-017-9794-8.
- 299 Hughes LC, Ortí G, Huang Y, Sun Y, Baldwin CC, Thompson AW, Arcila D, Betancur-R R, Li
300 C, Becker L, et al. 2018. Comprehensive phylogeny of ray-finned fishes (Actinopterygii) based
301 on transcriptomic and genomic data. *Proc Natl Acad Sci U S A*. 115(24):6249–6254.
302 doi:10.1073/pnas.1719358115.
- 303 Inoue J, Sato Y, Sinclair R, Tsukamoto K, Nishida M. 2015. Rapid genome reshaping by
304 multiple-gene loss after whole-genome duplication in teleost fish suggested by mathematical
305 modeling. *Proc Natl Acad Sci U S A*. 112(48):14918–14923. doi:10.1073/pnas.1507669112.
- 306 Jones DT, Taylor WR, Thornton JM. 1992. The rapid generation of mutation data matrices from
307 protein sequences. *Bioinformatics*. 8(3):275–282. doi:10.1093/bioinformatics/8.3.275.
- 308 Kaelin WG, Ratcliffe PJ. 2008. Oxygen sensing by metazoans: the central role of the HIF
309 hydroxylase pathway. *Mol Cell*. 30(4):393–402. doi:10.1016/j.molcel.2008.04.009.
- 310 Katoh K, Standley DM. 2013. MAFFT Multiple Sequence Alignment Software Version 7:
311 Improvements in Performance and Usability. *Mol Biol Evol*. 30(4):772–780.
312 doi:10.1093/molbev/mst010.
- 313 Katoh K, Standley DM. 2016. A simple method to control over-alignment in the MAFFT
314 multiple sequence alignment program. *Bioinformatics*. 32(13):1933–1942.
315 doi:10.1093/bioinformatics/btw108.
- 316 Kumar S, Stecher G, Li M, Knyaz C, Tamura K. 2018. MEGA X: Molecular Evolutionary
317 Genetics Analysis across Computing Platforms. *Mol Biol Evol*. 35(6):1547–1549.
318 doi:10.1093/molbev/msy096.
- 319 Lando D, Peet DJ, Gorman JJ, Whelan DA, Whitelaw ML, Bruick RK. 2002. FIH-1 is an
320 asparaginyl hydroxylase enzyme that regulates the transcriptional activity of hypoxia-inducible
321 factor. *Genes Dev*. 16(12):1466–1471. doi:10.1101/gad.991402.
- 322 Lynch M. 2002. Gene duplication and evolution. *Science*. 297(5583):945–947.
323 doi:10.1126/science.1075472.

- 324 Lynch M, Conery JS. 2000. The evolutionary fate and consequences of duplicate genes. *Science*.
325 290(5494):1151–1155. doi:10.1126/science.290.5494.1151.
- 326 Macqueen DJ, Johnston IA. 2014. A well-constrained estimate for the timing of the salmonid
327 whole genome duplication reveals major decoupling from species diversification. *Proc R Soc B*
328 *Biol Sci*. 281(1778):20132881. doi:10.1098/rspb.2013.2881.
- 329 Makino Y, Kanopka A, Wilson WJ, Tanaka H, Poellinger L. 2002. Inhibitory PAS domain
330 protein (IPAS) is a hypoxia-inducible splicing variant of the hypoxia-inducible factor-3alpha
331 locus. *J Biol Chem*. 277(36):32405–32408. doi:10.1074/jbc.C200328200.
- 332 McIntosh BE, Hogenesch JB, Bradfield CA. 2010. Mammalian Per-Arnt-Sim proteins in
333 environmental adaptation. *Annu Rev Physiol*. 72(1):625–645. doi:10.1146/annurev-physiol-
334 021909-135922.
- 335 Nikinmaa M, Rees BB. 2005. Oxygen-dependent gene expression in fishes. *Am J Physiol Regul*
336 *Integr Comp Physiol*. 288(5):R1079-1090. doi:10.1152/ajpregu.00626.2004.
- 337 Ohno S. 1970. *Evolution by gene duplication*. Berlin Heidelberg: Springer-Verlag.
- 338 Parey, E, Louis, A, Cabau, C, Gulgenn, Y, Crollius, HR, Berthelot, C. 2020. Synteny-guided
339 resolution of gene trees clarifies the functional impact of whole genome duplications. *Mol Biol*
340 *Evol*, doi.org/10.1093/molbev/msaa149
- 341 Pasquier J, Cabau C, Nguyen T, Jouanno E, Severac D, Braasch I, Journot L, Pontarotti P, Klopp
342 C, Postlethwait JH, et al. 2016. Gene evolution and gene expression after whole genome
343 duplication in fish: the PhyloFish database. *BMC Genomics*. 17:368. doi:10.1186/s12864-016-
344 2709-z.
- 345 Penn O, Privman E, Ashkenazy H, Landan G, Graur D, Pupko T. 2010. GUIDANCE: a web
346 server for assessing alignment confidence scores. *Nucleic Acids Res*. 38(suppl_2):W23–W28.
347 doi:10.1093/nar/gkq443.
- 348 Postlethwait JH, Woods IG, Ngo-Hazelett P, Yan YL, Kelly PD, Chu F, Huang H, Hill-Force A,
349 Talbot WS. 2000. Zebrafish comparative genomics and the origins of vertebrate chromosomes.
350 *Genome Res*. 10(12):1890–1902. doi:10.1101/gr.164800.
- 351 Powell WH, Hahn ME. 2002. Identification and functional characterization of hypoxia-inducible
352 factor 2alpha from the estuarine teleost, *Fundulus heteroclitus*: interaction of HIF-2alpha with
353 two ARNT2 splice variants. *J Exp Zool*. 294(1):17–29. doi:10.1002/jez.10074.
- 354 Ravi V, Venkatesh B. 2018. The divergent genomes of teleosts. *Annu Rev Anim Biosci*. 6:47–
355 68. doi:10.1146/annurev-animal-030117-014821.
- 356 Rojas DA, Perez-Munizaga DA, Centanin L, Antonelli M, Wappner P, Allende ML, Reyes AE.
357 2007. Cloning of hif-1alpha and hif-2alpha and mRNA expression pattern during development in
358 zebrafish. *Gene Expr Patterns GEP*. 7(3):339–345. doi:10.1016/j.modgep.2006.08.002.

- 359 Rytönen KT, Akbarzadeh A, Miandare HK, Kamei H, Duan C, Leder EH, Williams TA,
360 Nikinmaa M. 2013. Subfunctionalization of cyprinid hypoxia-inducible factors for roles in
361 development and oxygen sensing. *Evol Int J Org Evol*. 67(3):873–882. doi:10.1111/j.1558-
362 5646.2012.01820.x.
- 363 Rytönen KT, Williams TA, Renshaw GM, Primmer CR, Nikinmaa M. 2011. Molecular
364 evolution of the metazoan PHD-HIF oxygen-sensing system. *Mol Biol Evol*. 28(6):1913–1926.
365 doi:10.1093/molbev/msr012.
- 366 Sacerdot C, Louis A, Bon C, Berthelot C, Roest Crolius H. 2018. Chromosome evolution at the
367 origin of the ancestral vertebrate genome. *Genome Biol*. 19(1):166. doi:10.1186/s13059-018-
368 1559-1.
- 369 Sela I, Ashkenazy H, Katoh K, Pupko T. 2015. GUIDANCE2: accurate detection of unreliable
370 alignment regions accounting for the uncertainty of multiple parameters. *Nucleic Acids Res*.
371 43(W1):W7–W14. doi:10.1093/nar/gkv318.
- 372 Semenza GL. 2011. Oxygen sensing, homeostasis, and disease. *N Engl J Med*. 365(6):537–547.
373 doi:10.1056/NEJMra1011165.
- 374 Tarade D, Lee JE, Ohh M. 2019. Evolution of metazoan oxygen-sensing involved a conserved
375 divergence of VHL affinity for HIF1 α and HIF2 α . *Nature Comm* 10:3293.
376 doi.org/10.1038/s41467-019-11149-1
- 377 Townley IK, Karchner SI, Skripnikova E, Wiese TE, Hahn ME, Rees BB. 2017. Sequence and
378 functional characterization of hypoxia-inducible factors, HIF1 α , HIF2 α , and HIF3 α , from the
379 estuarine fish, *Fundulus heteroclitus*. *Am J Physiol Regul Integr Comp Physiol*. 312(3):R412–
380 R425. doi:10.1152/ajpregu.00402.2016.
- 381 Volff J-N. 2005. Genome evolution and biodiversity in teleost fish. *Heredity*. 94(3):280–294.
382 doi:10.1038/sj.hdy.6800635.
- 383 Waterhouse AM, Procter JB, Martin DMA, Clamp M, Barton GJ. 2009. Jalview Version 2--a
384 multiple sequence alignment editor and analysis workbench. *Bioinforma Oxf Engl*. 25(9):1189–
385 1191. doi:10.1093/bioinformatics/btp033.
- 386 Wheeler TJ, Clements J, Finn RD. 2014. Skylign: a tool for creating informative, interactive
387 logos representing sequence alignments and profile hidden Markov models. *BMC*
388 *Bioinformatics*. 15(1):7. doi:10.1186/1471-2105-15-7.
- 389 Wolfe, K. 2000. Robustness--it's not where you think it is. *Nat Genet* 25: 3-4.
390 doi.org/10.1038/75560
- 391 Zhang P, Yao Q, Lu L, Li Y, Chen P-J, Duan C. 2014. Hypoxia-inducible factor 3 is an oxygen-
392 dependent transcription activator and regulates a distinct transcriptional response to hypoxia.
393 *Cell Rep*. 6(6):1110–1121. doi:10.1016/j.celrep.2014.02.011.

394

395 **Box 1. HIF gene symbols**

396

397 Symbols for the hypoxia inducible factor alpha subunit follow the format:

398
$$\begin{pmatrix} HIF \\ hif \end{pmatrix} \begin{pmatrix} 1 \\ 2 \\ 3 \\ 4 \end{pmatrix} \begin{pmatrix} A \\ a \end{pmatrix} \begin{pmatrix} a \\ b \end{pmatrix}$$

399 Generally, the following conventions apply:

400

401 1. The Human Genome Consortium Gene Nomenclature Committee specifies that gene
402 symbols be all capital letters. The Zebrafish Nomenclature Conventions specifies
403 lowercase Latin letters for gene symbols. For other species, uppercase, lowercase, or
404 both have been used. The current study follows the convention for humans which has
405 been broadly applied to other vertebrates and invertebrates (e.g., Graham and
406 Presnell, 2017).

407 2. Paralogs that arose during two rounds of genome duplication at the base of vertebrate
408 evolution are indicated by Arabic numbers (1-4).

409 3. Because electronic databases are not uniformly compatible with Greek letters, Latin
410 letters (upper case in humans, lowercase in zebrafish) are used to distinguish the α
411 subunit from the β subunit, which was originally described as the aryl hydrocarbon
412 receptor nuclear translocator.

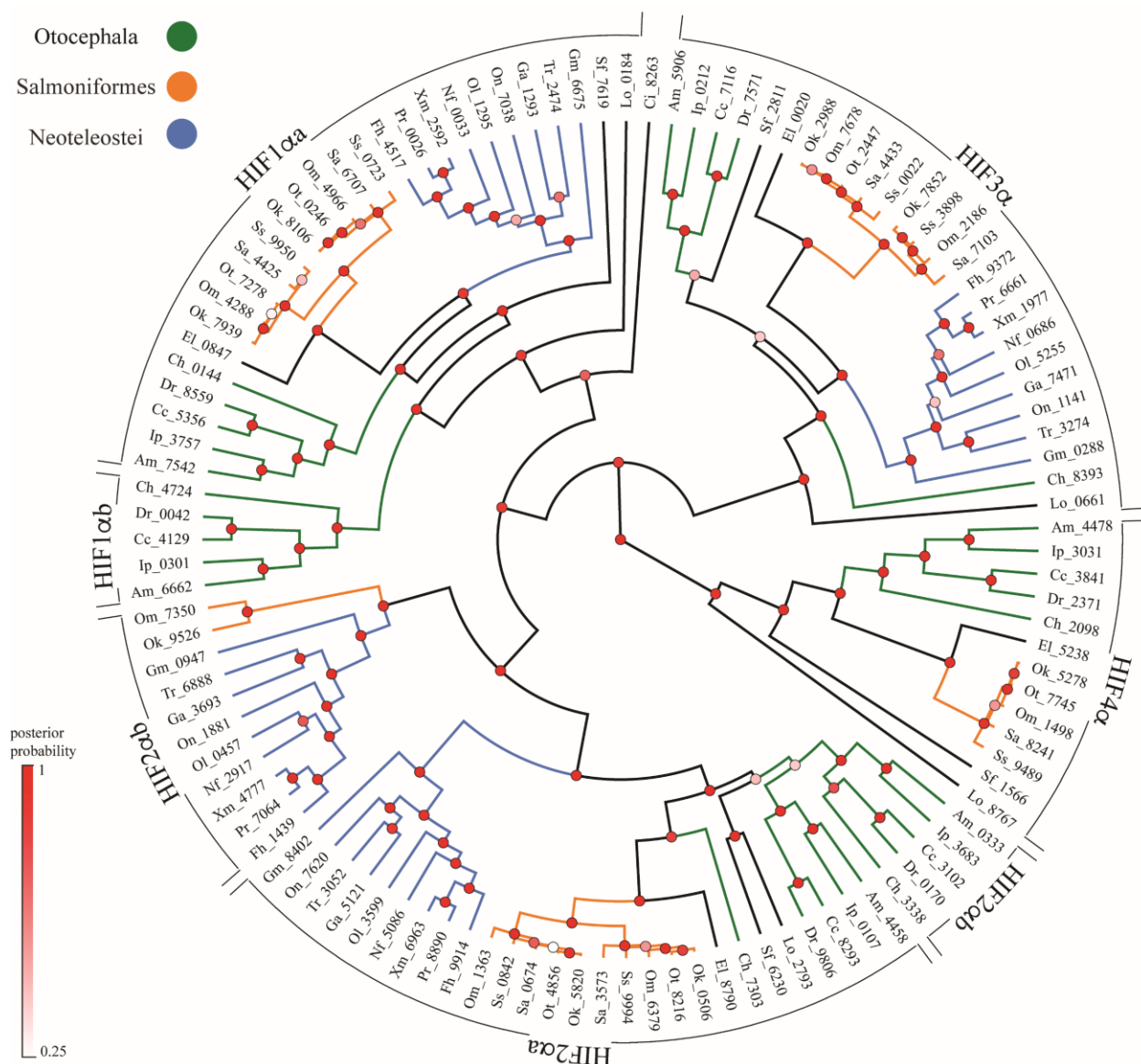
413 4. Paralogs that arose from the teleost-specific genome duplication are indicated by
414 lowercase Latin letters (a or b).

415 5.

416 Thus, the gene encoding the α subunit of the hypoxia inducible factor 1 is *HIF1A* in humans, but
417 the two paralogs in zebrafish that arose from the TGD are *hif1aa* and *hif1ab*. Also, because the α
418 subunit of the hypoxia inducible factor 2 was initially described as endothelial PAS-domain
419 protein, this gene is also known as *EPAS1* in humans and *epas1a* or *epas1b* in zebrafish.

420

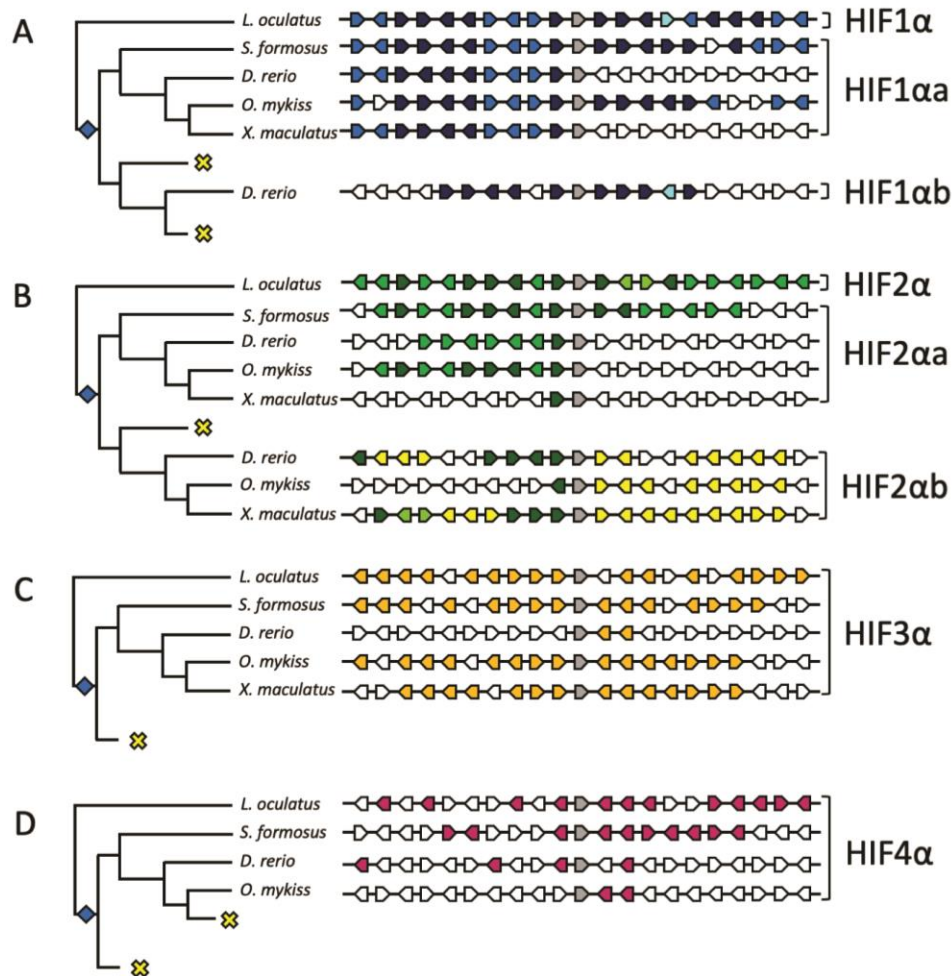
421



422

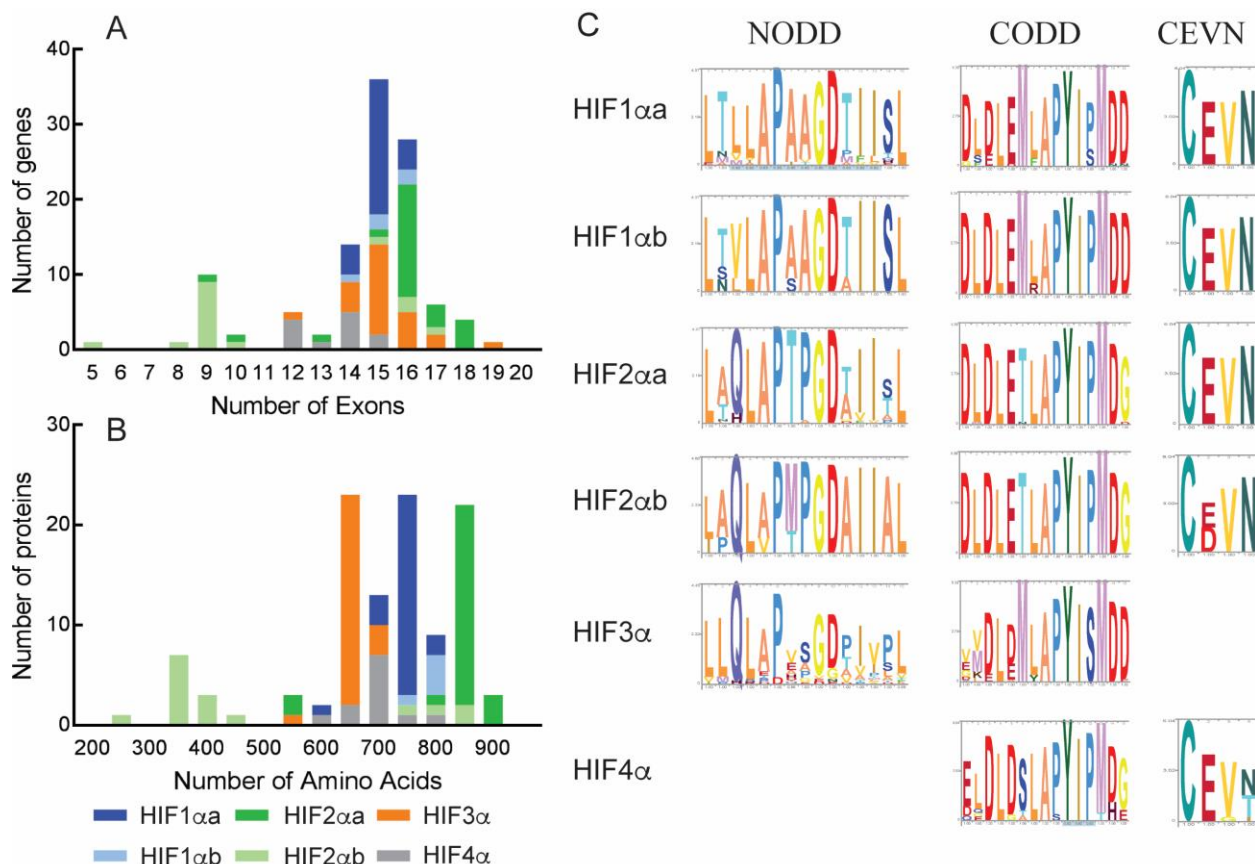
423

424 Fig. 1. Phylogeny of Actinopterygian HIF α reconstructed by Bayesian inference using full-length
 425 coding sequences. Analyses used the General Time Reversible model (GTR) with 6 gamma
 426 categories (+G) and allowing for invariants (+I). The tree with maximum clade credibility and
 427 mean heights is shown and the nodes are colored by posterior probability values. HIF α homology
 428 groups are shown on the periphery and the following taxa are color coded within each group:
 429 Otocephala (green); Salmoniformes (orange); Neoteleostei (blue). The outgroup, *Ciona*
 430 *intestinalis*, basal Actinopterygian (spotted gar, *Lepisosteus oculatus*), basal teleost (Asian
 431 arowana, *Scleropages formosus*), and sister taxa to Salmoniformes (Northern pike, *Esox lucius*),
 432 are not color coded. Sequences are identified by the first letter of the genus and species followed
 433 by the last four digits of the NCBI or Ensemble reference gene accession number (see
 434 supplementary table S1, Supplementary Material online for a full list of genes).



435

436 Fig. 2. Synteny analysis of Actinopterygian HIF1 α . The ten flanking genes on either side of each
 437 HIF α subunit (grey arrows) are compared among spotted gar (*L. oculatus*), Asian arowana (*S.*
 438 *formosus*), zebrafish (*D. rerio*), rainbow trout (*O. mykiss*), and southern platyfish (*X.*
 439 *maculatus*).
 440 A. Flanking genes shared between spotted gar HIF1 α and both HIF1 α paralogs in more derived
 441 fishes are shown as dark blue arrows, genes shared between spotted gar HIF1 α and HIF1 α a are
 442 shown as medium blue arrows, and genes shared between spotted gar HIF1 α and HIF1 α b are
 443 shown as light blue arrows. B. Flanking genes shared between spotted gar HIF2 α and both
 444 HIF2 α paralogs in more derived fishes are shown as dark green arrows, genes shared between
 445 spotted gar HIF2 α and HIF2 α a are shown as medium green arrows, and genes shared between
 446 spotted gar HIF2 α and HIF2 α b are shown as light green arrows. In addition, genes shared among
 447 HIF2 α b, but not present in spotted gar, are shown as yellow arrows. For HIF3 α (C) and HIF4 α
 448 (D), flanking genes shared between spotted gar and more derived species are shown as orange
 449 and purple arrows, respectively. The relationships among fishes is from Hughes et al (2018) and
 450 branch lengths do not indicate divergence times. The teleost-specific genome duplication is
 451 indicated by the blue diamonds, and putative losses of specific HIF α forms are shown by the
 452 yellow crosses. For abbreviations of flanking genes, see supplementary table S2, Supplementary
 Material online.



453
454

455 Fig. 3. Exon number (A), deduced protein length (B), and consensus sequences for putative
456 hydroxylation domains (C) for teleost HIF α subunits. Median values for exon number and amino
457 acid number were as follows: HIF1 α a = 15 exons, 759 amino acids (n=26); HIF1 α b, 15 exons,
458 777 amino acids (n=5); HIF2 α a, 16 exons, 853 amino acids (n=26); HIF3 α , 15 exons, 646 amino
459 acids (n=25); HIF4 α , 14 exons, 716 amino acids (n=12). For HIF2 α b, the distributions were
460 bimodal, with median values of 16 exons and 816 amino acids for Otocephala (n=5) and 9 exons
461 and 370 amino acids for other teleost (n=11). Exon number and deduced protein lengths for
462 individual sequences are shown in supplementary table S1, Supplementary Material online, and
463 summary statistics for major taxonomic groups are shown in supplementary table S3,
464 Supplementary Material online. Consensus sequences for the N- and C-terminal oxygen-
465 dependent degradation domains (NODD and CODD) and the C-terminal asparaginyl
466 hydroxylation motif (CEVN) were identified from multiple sequence alignments and visualized
467 with Skylign. The absence of a consensus sequence indicates that domain was not conserved for
468 the respective HIF α subunit. Data for spotted gar (*Lepisosteus oculatus*) are not included.